

# Effect of alloying additions on microstructure and properties of vertical-up MMA welds

## 2 — Results and discussion

Analysis and assessment of published data are carried out by **H K D H Bhadeshia** and **L-E Svensson** in presentation of their conclusions.

### STRENGTH

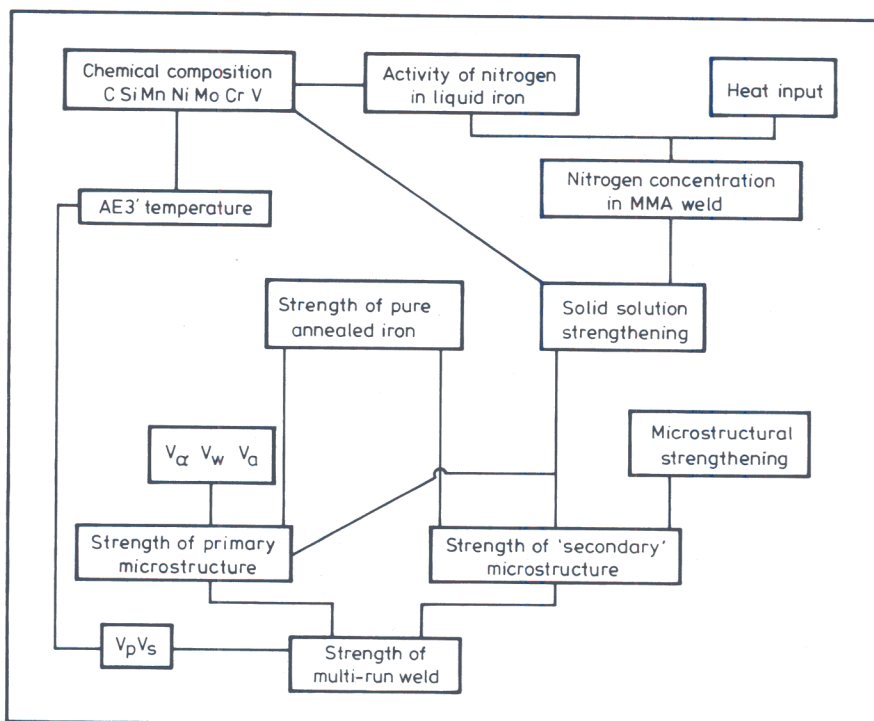
The procedure used is summarised in Fig. 4. Yield strength,  $\sigma_y$ , of a multi-run MMA weld deposit is given by<sup>10, 11</sup>

$$\sigma_y = V_p \sigma_p + V_s \sigma_s \quad \dots [14]$$

where  $\sigma_p$  is the yield strength of the primary microstructure, and is assumed additionally to approximate the strength of fully re-austenitised reheated regions.  $\sigma_s$  is the yield strength of regions which have largely lost the microstructural component of strength, and which are either partially re-austenitised or tempered. Recent work<sup>10</sup> has quantitatively resolved  $\sigma_p$  into components due to the strength of pure, annealed iron,  $\sigma_{Fe}$ , solid solution strengthening components,  $\sigma_{SS}$ , and microstructural strengthening components  $\sigma_{\alpha}$ ,  $\sigma_{\alpha_w}$  and  $\sigma_{\alpha_a}$ , due to  $\alpha$ ,  $\alpha_w$  and  $\alpha_a$ , respectively. Similarly,  $\sigma_s$  has been resolved into  $\sigma_{Fe}$ ,  $\sigma_{SS}$  and a component due to microstructural strengthening. Hence, both  $\sigma_p$  and  $\sigma_s$  can be estimated from a knowledge of the volume fractions of phases, alloy chemistry and readily available data on the strength of iron. It has been demonstrated that, using these procedures, the yield strength of the weld as a whole can be calculated with considerable accuracy for a wide range of alloy compositions and welding conditions.<sup>10</sup>

The solid solution strengthening term discussed above includes the effect of nitrogen concentration. In the calculations that follow, nitrogen concentration is

*Harshad Bhadeshia, BSc, MSc, CEng, is a lecturer in the Department of Materials Science and Metallurgy, University of Cambridge, and Lars-Erik Svensson is Research Manager at ESAB AB, Gothenburg.*



4 Procedure for estimating nitrogen content and strength of weld deposits.

in the absence of experimental data calculated using methods developed recently.<sup>11, 20</sup> It is recognised<sup>11, 20</sup> that these methods are crude, especially for MMA welds, where arc length, iron powder content, *etc* have not been taken into account. Furthermore, effects of dilution are not accounted for, although for all-weld metal deposits of the kind considered here this should not be an important factor. In spite of these difficulties it is possible to obtain a rough estimate of the

nitrogen concentration<sup>20</sup> of MMA weld deposits as a function of weld chemistry and heat input.

There is no model for prediction of MMA weld tensile strength. For the present work tensile strength,  $\sigma_U$ , is estimated empirically using the relation

$$\sigma_U = 112.4 + 0.9153 \sigma_y \text{ MPa} \quad \dots [15]$$

The relationship is derived by linear regression using yield strength data assessed in Ref. 11; the relationship has a correlation coefficient of 0.95.

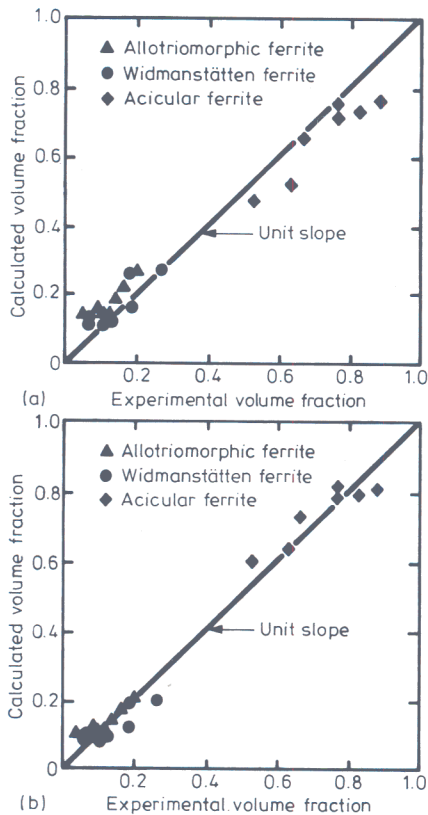
### RESULTS AND DISCUSSION

#### Assessment of published data

Comparison of calculated and experimental volume fractions of constituents in the primary microstructure (Fig. 5) was made for two types of austenite grain structure, first the *c* axes of the hexagonal prisms were assumed to be inclined at 66°

Joining & Materials research papers—denoted by page numbers with an R suffix—are subject to peer review under the auspices of our Editorial Advisory Panel. The panel members are:

Professor R L Apps, Cranfield Institute of Technology  
 Professor F M Burdekin, UMIST  
 Dr R E Dolby, The Welding Institute  
 Dr M J Whittle, CEGB

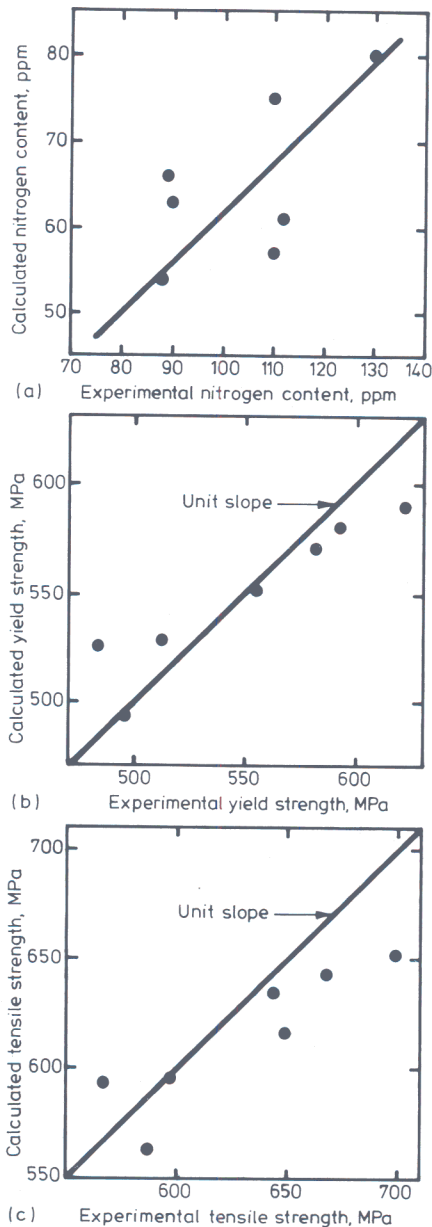


5 Comparison of calculated and experimental<sup>21</sup> volume fractions of phases for welds W5-W20: a) 66° angle between austenite grain c axes and welding direction; b) Zero angle.

to the normal of the transverse section<sup>25</sup> and second as a limiting case, the *c* axes were assumed to be exactly along the normal to the transverse sections of the welds. It is evident that there is good agreement between calculated and experimental data. This is strong evidence that variations in microstructure can be understood in terms of the influence of alloying additions on the kinetics and thermodynamics of transformations during continuous cooling heat treatment.

Comparison is made (Fig. 6) between estimated weld nitrogen concentration and the experimental data. While absolute agreement is poor, the method clearly gives the correct trend in nitrogen concentration as a function of alloy chemistry and heat input. It may be significant that calculated nitrogen concentrations which are based on welds deposited in the flat position consistently underestimate the nitrogen concentration of vertical-up welds, since these are positionally more difficult and in general involve longer arc length, conducive to greater nitrogen pick-up.

Results of strength calculations, carried out using the reported volume fractions of phases in the primary microstructure, showed that calculated yield strength was slightly underestimated at the highest strength values, although agreement with experimental data is good. Most of the variation in strength is directly attributable to changes in primary microstructure



6 Comparison of calculated and experimental<sup>21</sup>: a) Nitrogen concentration; b) Yield strength; c) Tensile strength, all for welds W5-W20.

and in  $V_p$  (Table 2, see Part 1), with the effect of solid solution strengthening being rather small. Court and Pollard<sup>21</sup> noted variations in acicular ferrite plate thickness ranging from about 1.19-1.92  $\mu\text{m}$ ; these do not represent the true plate thickness because of sectioning effects, but if it is assumed that variation in thickness is well represented by these data, then their influence on strength can be estimated. Daigne *et al* have shown that for lath martensite, the strength due to lath boundaries,  $\sigma_g$ , varies with lath thickness ( $\epsilon_1 \mu\text{m}$ ) as follows:<sup>46</sup>

$$\sigma_g \approx 116 \epsilon_1^{-1} \text{ MPa} \quad \dots [16]$$

On this basis, the reported variations<sup>21</sup> in acicular ferrite thickness should lead to a maximum change in strength of only 37MPa and may be neglected.

## General predictions

Presented in this section is a series of calculations of the microstructure, strength and other characteristics of MMA welds as a function of alloy chemistry and heat input. The results should be of use in design of welding consumables and procedures. The calculations are for MMA welds deposited in the flat position since, unlike vertical-up welds, austenite grain size can be estimated empirically:

$$\begin{aligned} \bar{L}_m (\mu\text{m}) = & 64.5 - 445.8(\text{wt}\% \text{ C}) \\ & + 138.6(\text{wt}\% \text{ Si}) - 7.591(\text{wt}\% \text{ Mn}) \\ & + 16 \times 10^{-6} Q (\text{J/m}) \quad \dots [17] \end{aligned}$$

It should be pointed out that the equation is derived from data in which silicon concentration varied between 0.27-0.41 wt%, and may consequently be unreliable during extrapolation outside that range. However, the trend is likely to be correct, especially since the extrapolation considered here is small.

Heat flow constants [7] used for the microstructure calculations are those appropriate to MMA welds deposited in the flat position:  $C_1=1325$  and  $C_2=1.6$ .<sup>3</sup>

Figure 7 shows that small variations in carbon concentration can have a major influence on weld microstructure, and this is especially so since the average carbon concentration of a weld (*i.e.*  $\bar{x}$ ) is usually kept low. The difference between solubility of carbon in ferrite,  $x^{\alpha\gamma}$ , and  $\bar{x}$  is therefore small, and transformation kinetics increase rapidly as the difference decreases, for two reasons. First, the supersaturation term which appears in most kinetic equations is given in [10] as

$$\Omega = (x^{\gamma\alpha} - \bar{x}) / (x^{\gamma\alpha} - x^{\alpha\gamma})$$

where  $x^{\gamma\alpha}$  and  $x^{\alpha\gamma}$  are the paraequilibrium carbon concentrations in austenite and ferrite, respectively, as obtained from the calculated phase diagrams, and  $\bar{x}$  is the average carbon concentration in the alloy. Thus, the driving supersaturation for growth increases as  $\bar{x}$  tends towards  $x^{\alpha\gamma}$ . Secondly, during diffusion controlled growth (*e.g.* for  $\alpha$  and  $\alpha_w$ ), the amount of carbon that has to be diffused ahead of the interface varies with  $(\bar{x} - x^{\alpha\gamma})$  and, as the latter tends to decrease to zero, diffusion controlled growth velocity increases sharply.

Hence the effect of carbon is seen to be largest when  $\bar{x}$  changes from 0.03→0.06 wt%, as compared with the change from 0.06→0.10 wt%. As will be seen later, the magnitude of changes in mechanical properties mimics this behaviour. It should also be noted that  $\alpha$  and  $\alpha_w$ , both of which grow with an equilibrium or paraequilibrium carbon concentration, are expected to exhibit similar behaviour with respect to carbon, observed to be so in Fig. 7. The behaviour seen for Fe-0.03C-0.35Si-Mn wt% alloys (and less obviously for the others), whereby the amount of acicular ferrite decreases with an initial increase in manganese concentration from 0.8-1.0 Mn



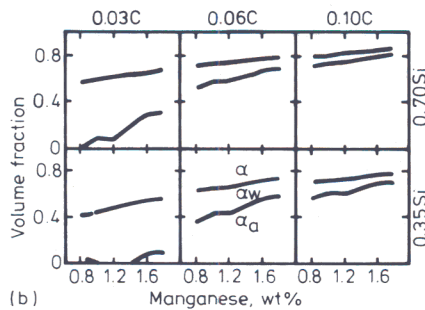
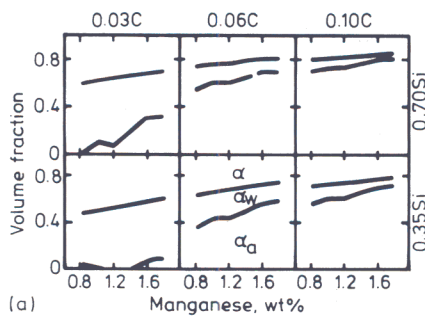
is a reflection of the accompanying decrease in austenite grain size as ( $\bar{L}_m$ ) decreases by about  $8\mu\text{m}$  per wt% increase in Mn concentration. This means that Widmanstätten ferrite grows right across the austenite grains before acicular ferrite has an opportunity to form. Otherwise, an increase in manganese concentration is generally seen to be beneficial to formation of acicular ferrite, reflecting a reduction in  $\alpha$  and  $\alpha_w$  with increasing concentration.

Silicon is known to increase the  $A_{e3'}$  temperature (Fig. 8) and the driving force for transformation. In spite of this, the experimental data and the authors' calculations indicate that it leads to a reduction in the volume fractions of  $\alpha$  and  $\alpha_w$ . This is because it increases  $\bar{L}_m$  and since nucleation of  $\alpha$  is essentially restricted to the  $\gamma$  grain boundaries, for a given value of allotriomorph thickness,  $V_\alpha$  must decrease with increasing  $\bar{L}_m$ . Note that for the same welding conditions the thickness of the layers of  $\alpha$  increases with Si but the volume fraction may decrease because of the change in  $\gamma$  grain size. In addition, there is relatively more austenite left for formation of acicular ferrite. Hence, for typical circumstances encountered in MMA welding, an increase in silicon concentration from 0.35–0.70 wt% leads to an increase in the amount of acicular ferrite at the expense of  $\alpha$  and  $\alpha_w$ . It should however be noted that thicker layers of allotriomorphic ferrite make for poorer toughness, in spite of the beneficial effect of silicon on the volume fraction of acicular ferrite, so that silicon is not recommended as an element for improvement of toughness beyond that necessary for good deoxidation practice.

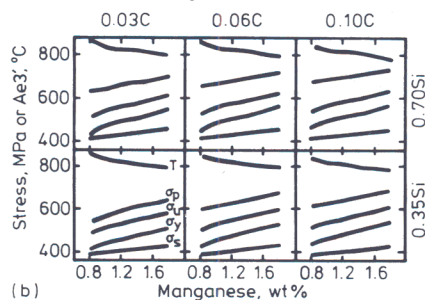
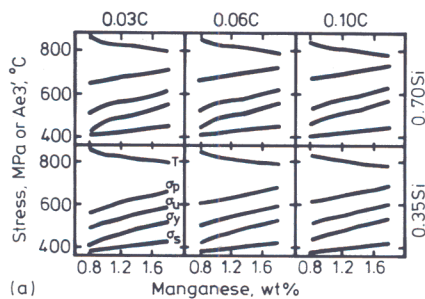
An increase in the heat input from 1.0–1.4 kJ/mm causes a relatively small change in microstructure, tending to reduce the amount of acicular ferrite, consistent with a lower cooling rate giving more opportunity for growth of  $\alpha$ . Widmanstätten ferrite, which through its rapid rate of growth forms virtually isothermally, is not much affected by the lower cooling rate associated with higher heat input. The relatively small effect of heat input is considered beneficial because uncontrolled variations are inevitable during MMA welding.

The expected trends in nitrogen concentration are illustrated in Fig. 9. Consistent with the thermodynamics governing the solution of nitrogen in liquid iron, carbon and silicon have the opposite effect compared with manganese, which causes an increase in weld metal nitrogen concentration. An increase in heat input also leads to increase in weld nitrogen content. It is emphasised that the procedure<sup>11,20</sup> for calculation of nitrogen concentration in MMA welds is weak and the results should be taken as an indication of trends in total nitrogen content, rather than a prediction of the absolute values.

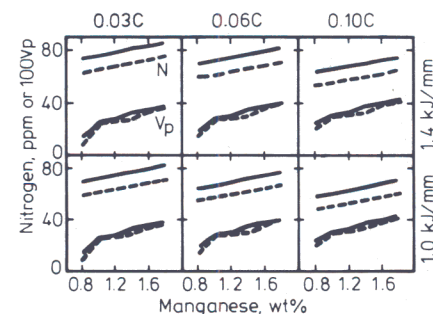
Figure 9 also shows the variation in  $V_p$ ,



7 Primary microstructure calculation for series of hypothetical welds deposited in flat position at heat input of: a) 1.0 kJ/mm; b) 1.4 kJ/mm.



8 Calculation of  $A_{e3'}$  temperature and strength of welds represented in Fig. 7 at heat input of: a) 1.0 kJ/mm; b) 1.4 kJ/mm.



9 Calculation of nitrogen concentration and  $V_p$  for welds represented in Fig. 7. Dashed line=1.4 kJ/mm, continuous line=1.0 kJ/mm.

which increases with manganese and carbon concentration and decreases with silicon concentration in accordance with the effect of these elements on the  $A_{e3'}$  temperature (Fig. 8). A higher value of  $V_p$  leads to higher net strength since the as-deposited microstructure has the highest strength of all the constituents of a multi-run weld (Fig. 8, 9). Note that the variation of  $\sigma_p$  as a function of alloy chemistry is greater than would be caused by solid solution strengthening, since the mixture of  $\alpha$ ,  $\alpha_w$  and  $\alpha_a$  also alters with alloy chemistry and heat input. On the other hand, the microstructural strengthening component in  $\sigma_s$  is small, much of its variation being a reflection of solid solution strengthening. This is the major reason for the difference in slope of the  $\sigma_p$  and  $\sigma_{ss}$  curves presented in Fig. 8. Because of the large difference in  $\sigma_p$  and  $\sigma_{ss}$ , the variation of  $\sigma_Y$  with alloy chemistry, etc, depends largely on that of  $\sigma_p$ .

## Conclusions

It has been demonstrated that given the austenite grain structure, reported variations in microstructure and strength of vertical-up MMA welds, as a function of alloy chemistry and heat input, are largely explained using phase transformation theory and recent work on mechanical properties of weld deposits. More research on the morphology of austenite grains in vertical-up welds and on factors controlling their size and shape is needed before a more nearly complete prediction of microstructure and properties can be attempted. Systematic data on nitrogen content of vertical-up welds and consumables used in their manufacture would also be valuable in refining methods for predicting nitrogen concentration.

## Acknowledgements

The authors are grateful to ESAB AB (Sweden) for financial support and for provision of laboratory facilities, and to Professor D Hull for provision of laboratory facilities at the University of Cambridge.

## J&M FILE

Authors Bhadeshia H K D H and Svensson L-E

Title Effect of alloying additions on microstructure and properties of vertical-up MMA welds.

Reference Joining & Materials 1989 2 (4) 182R-187R, and (5) 236R-238R

The metallurgical principles and mathematical methods involved in calculation of weld microstructures from chemical composition, heat input, joint design, etc, are explored with a view to extending flat position models to the vertical-up position and theoretical design of weld deposits without much experimental work. Areas explored are prediction of primary microstructure, austenite grain structure, cooling conditions, and calculation of primary microstructure. The problem of calculation of secondary microstructure is mentioned. Topics include solidification microstructure, transformation, thermal cycles of welding and heat treatment, and effects of composition.